scientific data

Check for updates

OPEN

DATA DESCRIPTOR

Dataset of human skin and fingernails images for non-invasive haemoglobin level assessment

Boris Yakimov[1,2,3] ✉, Kirill Buiankin[1], Georgy Denisenko[2], Ilia Bardadin[1], Oleg Pavlov[1], Yuliya Shitova[4], Alexey Yuriev[3], Lyudmila Pankratieva[3], Alexander Pukhov[3], Andrey Shkoda[3] & Evgeny Shirshin[1,2] ✉

Anaemia, a decrease in total concentration of haemoglobin (Hb) in blood, affects substantial percentage of the population worldwide. Currently, the gold standard for determining the Hb level is the invasive analysis of venous blood. Yet, more and more research groups demonstrate the possibility of non-invasive Hb assessment using white light imaging of tissue sites where Hb is the main chromophore, in particular, fingernails. Despite the promising declarations, non-invasive Hb assessment via RGB-imaging is still poorly used in practice. The main reason is the difficulty in establishing the true accuracy of the methods presented in different works since they are tested on private datasets collected under different experimental conditions. Here we present an open dataset containing RGB images of skin and fingernails for patients with a known level of Hb, thus providing a single benchmark for researchers and engineers in the field, aimed at fostering translation of non-invasive imaging methods to the bedside.

Background & Summary

Overview of data collection goals. Haemoglobin (Hb), the main protein in the human blood, is responsible for oxygen transport in the organism. The total Hb concentration in blood (hereinafter referred to as Hb level) is a significant clinical parameter. Anaemia, i.e. a decrease of the Hb level, affects approximately 29% of non-pregnant women, 38% of pregnant women and 43% of children[1–3]. Undiagnosed or improperly treated anaemia can lead to adverse outcomes for the newborns, increased risk of complications, and reduce quality of life[4,5].

The gold standard for Hb assessment is the invasive venous blood sampling followed by standard assays[6]. Such an analysis requires qualified personnel for biomaterial sampling, certified laboratory equipment, and, most important, it is costly, time-consuming, and hurtful for the patient[6]. Thus, non-invasive methods allowing for immediate and painless determination of the Hb level are of high demand.

Since Hb is the dominant chromophore in the human organism, most of the suggested non-invasive methods for its assessment are based on the estimation of light attenuation in various tissues sites. The measured light attenuation is then calibrated according to the Hb level obtained using the reference (invasive) techniques. Generally, to achieve high accuracy of non-invasive Hb assessment, imaging is performed for the tissue sites where the impact of melanin, the skin pigment responsible for its brown colour, is negligible. The state-of-art results in non-invasive Hb assessment are summarized in Table 1.

The first class of works report on the possibility of non-invasive Hb determination from the RGB images of the eye palpebral or bulbar conjunctiva, yielding the standard error of ~15–20 g/L[7–14], and some of them present datasets with raw images[8,10,12]. The second class of works demonstrate the possibilities of non-invasive prediction of blood parameters using images of the fundus and external eye[15–17]. Some of them include a large number of patients involved (10^4–10^5) and provide a ~10 g/L standard error of the Hb level assessment[15] and the anaemia prediction with F-score of 0.8[16,17]. Yet, training of models in these works was carried out on unbalanced datasets, where most of the Hb levels exceeded 110 g/L, i.e., were close to the normal values. Moreover, the conjunctiva

[1]Faculty of Physics, M.V.Lomonosov Moscow State University, 1-2 Leninskie Gory, 119234, Moscow, Russia. [2]Laboratory of Clinical Biophotonics, Biomedical Science and Technology Park, Sechenov First Moscow State Medical University, Trubetskaya 8, Moscow, 119048, Russia. [3]Moscow State Budgetary Institution of Healthcare "L.A. Vorohobov City Clinical Hospital No. 67 MHD", Moscow, Salama Adil str., 2/44, 123423, Russia. [4]Medeum LLC, Vysokovoltny proezd 1/20, Moscow, 127566, Russia. ✉e-mail: bp.jakimov@physics.msu.ru; eshirshin@gmail.com

№	Number of patients involved	Online availability meta-	raw data	Best 95%-limits of agreement, g/L (−2SD, 2 SD)	(min, max) Hb range g/L	Tissue site	Reference
1	344	Yes	No	(−42, 44)	(47, 196)	Conjunctive	[7]
2	710	Yes	Yes	(−35, 36)	(31, 150)	Conjunctive	[8]
3	1065	No	No	(−37, 37)[1]	(60, 180)	Conjunctive	[9]
4	218	Yes	Yes	—	(70,174)	Conjunctive, sclera	[10]
5	117	No	No	(−54, 54)[4]	(43,182)	Conjunctive	[11]
6	218	Yes	Yes	—	(70, 174)	Conjunctive	[12]
7	94	No	No	(−34,34)[5]	(66,161)[5]	Conjunctive	[13]
8	153	No	No	(−22, 23)	(45, 190)	Conjunctive	[14]
9	57163	Yes	Yes	(−18,19)	(80, 175)	Fundus	[15]
10	14814	No	No	(−19, 18)	(60,180)	Fundus	[16]
11	38398	No	No		—	External eye	[17]
12	1216	Yes	No	(−25, 30)	(77, 192)	Fingertip	[19]
13	148	No	No	(−48, 15)	—	Fingertip	[20]
14	440	No	No	(−23,21)	(80,180)	Fingertip	[21]
15	122	No	No	(−22,39)	(90, 176)	Fingertip	[22]
16	299	No	No	(−37, 28)	(80,180)	Fingertip	[3]
17	35	No	No	(−30, 19)	(60,160)	Fingertip	[23]
18	677	No	No	(−43, 30)	(60, 180)	Fingertip	[24]
19	100	No	No	(−24, 24)	(60,160)	Fingernail	[35]
20	353	No	No	(−11, 11)	—	Fingernail	[36]
21	220	No	No	(−10,10)	—	Fingernail	[37]
22	35	No	No	(34,−34)	(80, 120)	Fingernail	[25]
23	131	No	No	(−15,15)	(77, 158)	Fingernail	[38]
24	138	No	No	(−15,15)	(85, 135)	Fingernail	[39]
25	710	Yes	Yes	—	—	Fingernail, conjunctive, palm	[40]

Table 1. The performance of non-invasive methods for the Hb level assessment. Best 95%-limits of agreement denote the range where 95% of all deviations of predicted Hb level from the true values belong for the best model among models presented in the work.

and the fundus are hard to reach tissue sites, and their imaging still requires special equipment and is not comfortable for the patient.

The most accessible melanin-free site for optical non-invasive Hb assessment is the fingernails region. Several commercially available devices that are worn on the fingertip allow non-invasive assessment of the Hb level using multispectral photoplethysmography[18]. Although such devices are approved by the Food & drug administration (FDA) and have already been introduced into clinical practice, independent comparisons with the reference method show that their error is ~20 g/L, i.e., comparable to imaging-based techniques[3,19–24].

The third class of works in Table 1 is based on the fingernails imaging. In 2018 Manino *et al.* demonstrated the possibility of determining the Hb level with an error of ~10–15 g/L by analysing RGB images of fingernails obtained with a smartphone[25]. Hence, the nails colour was shown to be prospective for determining the Hb level in blood. This observation stimulated numerous attempts to build a clinically reliable imaging method for Hb level assessment. Despite dozens of papers discussing this idea and even the existence of iOS and Android applications implementing it, non-invasive assessment of Hb level via RGB-imaging of fingernails is still poorly used in practice. The main reason is the difficulty in establishing true accuracy of the methods presented in different works caused by the fact that different authors (1) tend to create and test their algorithm on their private datasets collected under various experimental conditions; (2) use different metrics in assessing the accuracy of their algorithm; (3) use different methods for validation of the model. Here we present an open dataset containing RGB images of hand areas with nail plates for patients with a known level of Hb, thus providing a single benchmark for researchers and engineers in the field aimed at fostering translation of non-invasive imaging methods to the bedside.

General dataset description. To create a dataset of RGB images of skin and fingernails for non-invasive haemoglobin level assessment we've simultaneously imaged the patients' fingers with clearly visible nail plates without artificial coatings, damaging and discoloration under controlled illumination conditions. For all subjects the Hb level was determined using the invasive procedure and a certified haematological analyser. Details of the performed imaging setup are presented in the Methods section.

Examples of the obtained RGB-images for hands of patients with different Hb levels are shown in Fig. 1a. Additionally, we manually segmented the images of the nail plates and areas of the skin of the hand to facilitate image preprocessing for further analysis (Fig. 1b).

The data were collected for 250 patients with known Hb levels. The dataset was balanced by gender and contained 128 male and 122 female patients (Fig. 2a). The sample included patients of different age. The average

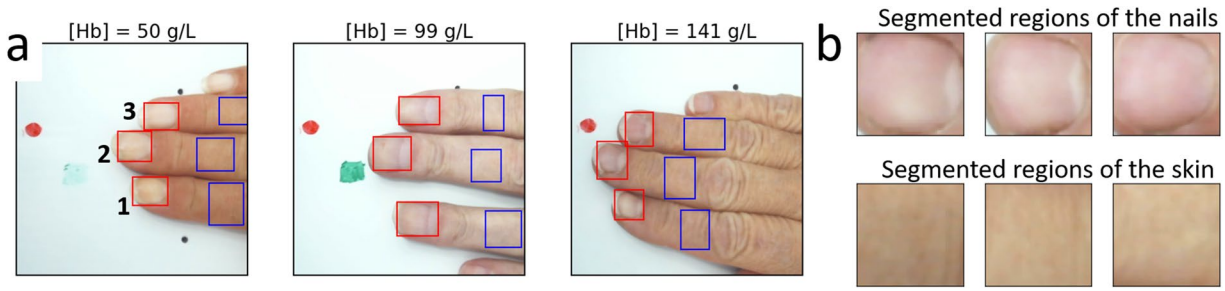

Fig. 1 (**a**) Exemplary images of hands presented in the dataset for patients with different total blood haemoglobin level (**b**). An example of segmented areas of nail plates and skin areas.

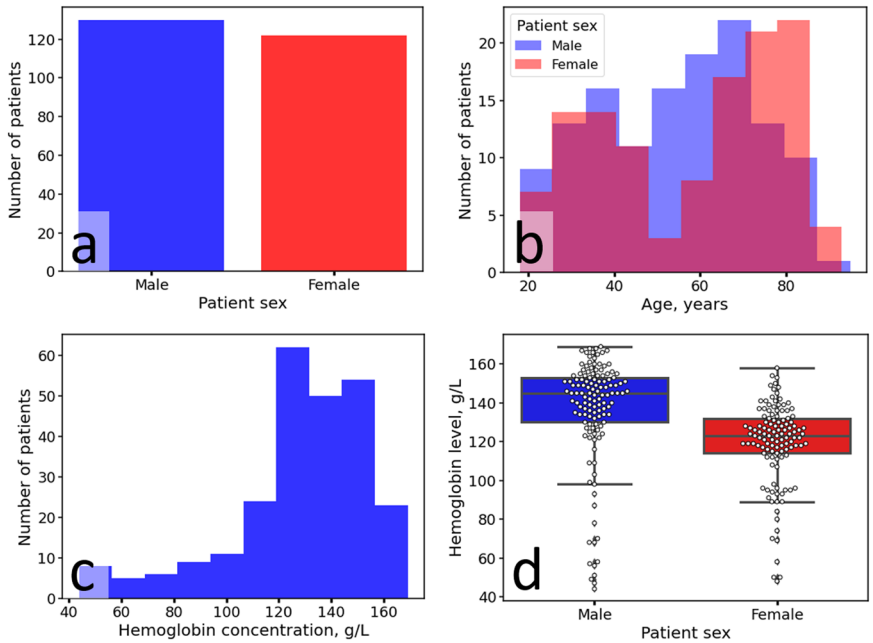

Fig. 2 (**a**) The number of male and female patients presented in the dataset. (**b**) The age distribution for patients of different gender in the dataset. (**c**) Distribution of the total Hb level estimated using the certified (invasive) procedure. (**d**) Boxplots of the total Hb level for male and female patients.

Gender	Mean Age	SD	Min. age	25%-percentile	Median age	75%-percentile	Max. age
Female	58.2	21.5	18	38	65	76	93
Male	54.2	18.4	18	40	56.5	69	95

Table 2. Descriptive statistics on the age (in years) distribution of subjects participating in the study.

age was 56 ± 20 y.o. spanning from 18 to 95 y.o. (Fig. 2b). Statistical parameters describing the distribution of patients' age are presented in Table 2.

The dataset included both patients with the Hb levels in the normal range and with low Hb levels. The Hb level distribution with and without split by gender is shown in Fig. 2c,d. Descriptive statistics of the Hb level distribution is also presented in Table 3. In total, 69 patients with Hb levels below 120 g/L were present in the sample.

We also assessed the distribution of patients with various skin tones (Fitzpatrick skin types) in the dataset, considering that the presence of melanin, another dominant skin chromophore, could potentially impact the accuracy of non-invasive Hb level assessment. To determine the distribution of patients with different skin tones (Fitzpatrick skin types) in our dataset, we assessed individual typology angle[26], which allows categorizing individuals based on their skin tones from very light (Fitzpatrick skin type I) to dark (Fitzpatrick skin type VI) using L*a*b* color coordinates of the segmented skin regions. The distribution of patients with different skin tones in the dataset is presented in Table 4.

Gender	Mean concentration	SD	Min. level	25%-percentile	Median level	75%-percentile	Max. level
Female	119	21.5	48	114	123	131.8	158
Male	136	28.6	44	129.8	145	153	169

Table 3. Descriptive statistics on the distribution of the Hb level, determined by performing a complete blood count.

Skin tone (Fitzpatrick type)	Very light (FP I)	Light (FP II)	Intermediate (FP III)	Tanned (FP IV)	Brown (FP V)
Number of patients	90	89	44	21	6

Table 4. Distribution of the number of patients in the dataset by skin tonalities (skin type).

Methods

Invasive determination of the Hb level was carried out according to standard clinical protocols[27,28]. Venous blood collected from the antecubital vein using the Vacutainer was characterized using the CBC analysis in a certified (ISO 15189:2012) clinical diagnostic laboratory. The measurements were performed 10–15 minutes after imaging of a patient's hand.

A special experimental setup was developed to obtain images under standardized illumination conditions. The setup consisted of a ~40 × 40 × 20 cm box made of aluminium composite material, inside which a Logitech C615 USB-camera and white LED illuminator providing colour temperature of ~7300 K were mounted. The box had a rectangular slot with the size of ~15 × 10 cm, so the patient could put his hand. After that, the image was taken under standard conditions with the exposure time, illumination conditions and image resolution fixed for all patients. In order to prevent the appearance of undesirable artefacts, two to three photographs of each patient's hands were taken. After that, the most successful image was selected and placed it in the dataset to avoid redundancy.

The measurements were carried out in the admission department of the L.A. Vorokhobov City Clinical Hospital No. 67 (Moscow, Russia). All patients gave their informed consent to participate in the study and to the open publication of the data. The study was approved by the Moscow City Ethics Committee on the basis of the Regulations on the City Ethics Committee and in accordance with the standards of operating procedures (Protocol No. 68 dated July 4, 2022).

Data Records

The data record has been deposited at *figshare*[29]. All data are presented in an anonymized form and do not contain direct or indirect patients' identifiers according to guidlines[30]. The 'metadata.csv' file contains a table, each line of which contains the following patient information:

- PATIENT_ID – identification number of the patient in the dataset;
- MEASUREMENT_DATE – hashed string corresponding to the measurement date;
- HB_LEVEL_GperL – the patient's Hb level, determined using a certified haematology analyzer, in g/L.
- NAIL_BOUNDING_BOXES– [[top_1, $left_1$, $bottom_1$, $right_1$], …, [top_3, $left_3$, $bottom_3$, $right_3$]] a list of lists of four integer values representing the coordinates of the upper left corner and lower right corner of the rectangle framing the patient's nails in the image;
- SKIN_BOUNDING_BOXES – [[top_1, $left_1$, $bottom_1$, $right_1$], …, [top_3, $left_3$, $bottom_3$, $right_3$]] a list of lists of four integer values representing the coordinates of the upper left corner and lower right corner of the rectangle framing the patient's skin areas.

For the lists of coordinates of nails and skin areas of the finger, the following conventions are applicable. Index 1 always corresponds to the index finger, index 2 to the middle finger, index 3 to the ring finger of the measured hand (Fig. 1b).

The 'photo' folder contains photographs taken for each patient. The files have the format 'photo/{PATIENT_ID}.jpg', for example, the file 'photo/11.jpg' corresponds to a patient with PATIENT_ID = 11 presented in 'metadata.csv' table.

Technical Validation

Blood collection and reference method for determining Hb level. Quality of haemoglobin reference values is guaranteed by adhering to the standard protocols and guidelines for clinical blood sampling carried out by qualified medical personnel[27,28]. Determination of the Hb level in venous blood was carried out using a certified haematological analyser in the ISO 15189:2012 standardized clinical diagnostic laboratory of the City Clinical Hospital No. 67 (Moscow, Russia).

Assessment of the image quality. Imaging was performed under fixed illumination conditions in an isolated box excluding external light. The exposure time and white balance on the camera were chosen so that the intensity of the reflected light in the areas corresponding to the nail and skin areas of the hand fell into the dynamic range of the camera, i.e., areas of interest corresponding to the nail plate and skin did not exhibit intensity values close to 255 or to zero. The intensity histograms for all areas of interest corresponding to the nail and skin are shown in Fig. 3a,b.

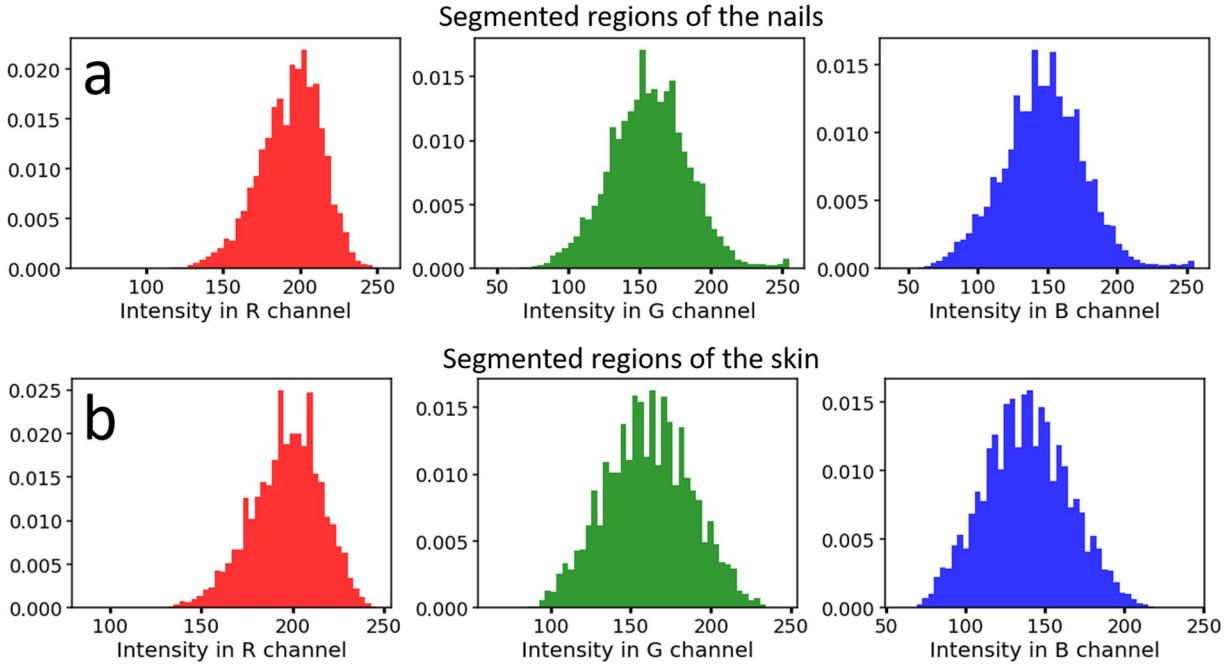

Fig. 3 Intensity distributions in R, G and B channels of segmented regions of the nails (**a**) and finger skin (**b**) calculated for the whole dataset.

Illumination stability. Additionally, to control for illumination stability, the average intensity in the image area corresponding to a white reference of 50 × 50 pixels with coordinates of the upper left corner (X = 300, Y = 350) in R, G, B color channels were calculated. The mean intensity in R, G, B were constant with deviation of no more than 3% from the mean intensity in dataset. The illumination LED-source color temperature was characterized using the method proposed in Hernandez-Andres *et al.*[31] to assure its constancy in images of the dataset. The color temperature in the images of the dataset in the reference area was constant and equal to ~7300 ± 170 K, i.e. varied with relative deviation of no more than ~2.5% across images of the dataset (Fig. 4).

Image segmentation. Nail plates can be segmented using semi-automatic methods, however, for a more reliable verification, we performed all segmentation manually using the ImageJ (the ROI Manager plugin)[32]. All bounding boxes were made to meet the following criteria. In the case of segmentation of the nail plate, the coordinates of the bounding box were chosen so that the bounding box included the nail plate completely. In the case of segmentation of a skin area, an intact skin without any visible pigmentation on the intermediate phalanx of the fingers was selected by the bounding boxes. Segmentation was performed in a randomized order by one specialist (B. I.) and additionally verified independently (Y.B., S.E.).

Usage Notes

In this section we demonstrate the possibility of building the simplest machine learning model to predict total Hb level in blood based on the data presented above, including the steps of raw image preprocessing, feature extraction, model tuning and evaluation on hold-out validation and test sets. We also provide the code written in the interactive JupyterNotebook environment in Python3 to ease the data-preprocessing steps and speed up one's own hypotheses testing using the presented data. This section does not claim models with the highest accuracy, but rather demonstrates the finished implementation of model-building pipeline.

We started our model implementation from the feature extraction from raw images presented in the dataset (Fig. 5a). First, the regions containing fingernails (red bounding boxes in Fig. 5a) and homogenous skin regions (blue bounding boxes) of the hand were extracted for each patient. We also segmented the region with the white background to normalize the intensities of the RGB images of the nails and skin to assure independency of the image intensities on the illumination.

As segmented image crops of fingernails could partially include areas that did not correspond to nail plates, central areas of the cropped nails and skin regions of the 60% width and height of initial crop were selected, as it is shown in Fig. 5b by dashed rectangles. For the selected inner regions the values of the 5-, 15-, 25-, 50-, 75-, 85- and 95- percentile levels of the intensity distribution for the R,G and B channels were calculated (42 features in total). For simplicity, we only used information from the middle finger for all volunteers. Obviously, additional verification of the model and increase in accuracy can achieved by using the information from several fingers by averaging the prediction results or using other aggregation methods. The obtained intensity values were then normalized to the median of RGB intensities of the white background region. The resulting 42 descriptors for all 250 patients were used as input features for training machine learning algorithms to predict the Hb level.

Since for classical machine learning algorithms it is highly desirable that the high and low target values are almost uniformly presented in the training dataset, the data were additionally balanced. To balance the sample

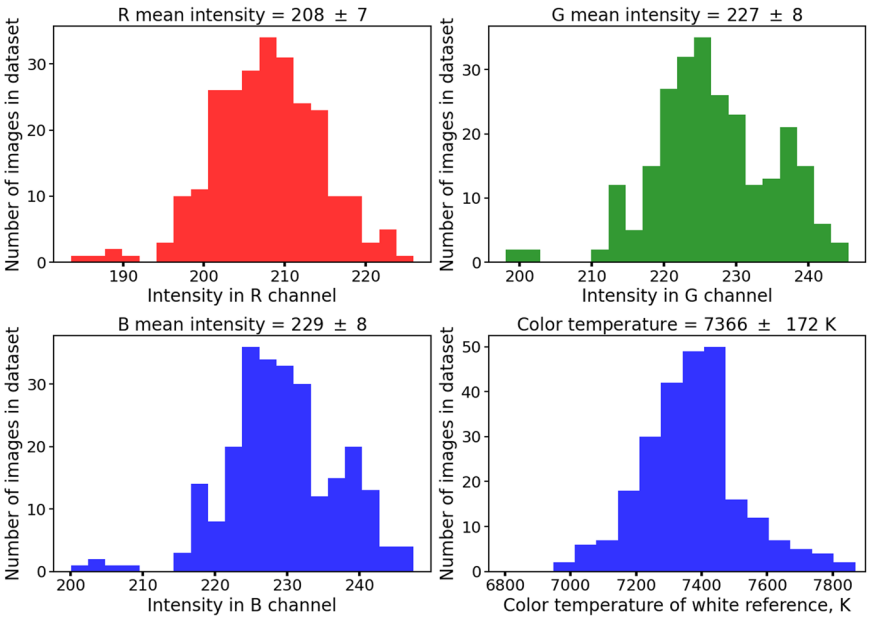

Fig. 4 Intensity distributions of mean R, G, and B channels and correlated color temperature of the white reference standard in images of the dataset.

we implemented custom under-sampling strategy. To perform subsampling the empirical probability density function p of the Hb level was fitted using the kernel density estimation method with Gaussian kernel with bandwidth of 0.5 g/L (Fig. 5c), and then 100 observations were sampled without replacement from the dataset with a probability for each point proportional to $\sim 1/p$, (i.e. one patient could be presented in the subsampled dataset only once). Thus, less presented Hb level values would be sampled with higher probability (Fig. 5d). The balancing procedure led to the fact that nearly 44% of observations in the balanced dataset fell into the Hb level region of $<$120 g/L instead of 28% values in the initial dataset (Fig. 5e).

As the next step the quality metrics and model validation procedure were chosen. The root mean squared error (RMSE) was used to evaluate the model accuracy, while the model validation was performed in a two-step way: the selection of model hyperparameters was carried out using 7-fold cross-validation on a selected balanced subset of 100 patients, and the final model testing was performed on patients not included in the balanced train dataset.

For demonstration, linear regression was used to predict the Hb level from the extracted features. Since some features were correlated with each other, to eliminate the "redundant description", we used a modification of linear regression with L_1 and L_2 regularization (the so-called Elastic Net model[33]), where the ratio between L_1 and L_2 regularization ($l_1 -$ ratio) and the contribution of the regularization term to the loss function (α) were optimized using exhaustive search over the grid of the hyperparameters. We varied the $l_1 -$ ratio on the grid of five values ($l_1 -$ ratio $= \{0.01,\ 0.1,\ 0.5,\ 0.9,\ 0.99\}$), while the α parameter varied on the logarithmic grid from 10^{-4} to 10^4 with 50 steps. The best hyperparameters for the Elastic Net model implemented in the Scikit-Learn library[34] were found to be equal to $l_1 -$ ratio $=\ 0.9$ and $\alpha \approx 0.2$.

The results of the best model predictions on the validation and test sets are presented in Fig. 5f–h. It can be seen that the model built on the validation set generalizes well to the test data, but slightly overestimates the values in the range of low Hb levels (Fig. 5f,g). The overall model error in terms of RMSE was equal to 24 g/L on the validation data set and 20 g/L on the test data set. The lower error on the test dataset can be explained by the fact that the true values of the Hb level in the test dataset are mainly localized in the normal Hb level range. As indicated earlier, the train/validation dataset was constructed to be balanced in terms of reference Hb levels to include both low and high reference values of Hb: the average Hb level in the balanced subset was 119 g/L with a standard deviation of 35 g/L. The additional test set included all other patients not included in the balanced subset. Thus, in this test set, most of the observations were concentrated in the range of normal hemoglobin levels, with a mean Hb level of 135 g/L and a standard deviation of 17 g/L. Therefore, the higher error in the validation set can be explained by both a large spread of reference Hb levels and a shift of reference values to a lower range.

We also evaluated RMSE of Hb level prediction broken down by different skin tonalities. Since in our dataset the number of patients with Fitzpatrick skin types I and II was dominant, while tanned skin types (FPIII – FPV) were less represented (Table 4), we decided to compare the Hb level prediction error for the following groups: FP I (90 individuals), FP II (89 individuals), and a combined group "FP III-V", which included patients with skin types from FP III to FP V (71 individuals). We retained the splits into validation and test sets used to assess the quality of models previously. We observed that RMSE values of Hb prediction did not vary significantly by skin type — only in the case of the Very Light skin tone (FP I) group in the validation dataset, the error of Hb level prediction was 26 g/L, while for groups FP II and FP III-V it was 22 g/L and 21.5 g/L, respectively. On the test sample, the Hb level errors were 19, 21.3, and 20.8 g/L for the FP I, FP II, and FP III-V groups, respectively. These results corroborate the hypothesis that the use of melanin-free nail plate data helps to avoid bias in predictions of

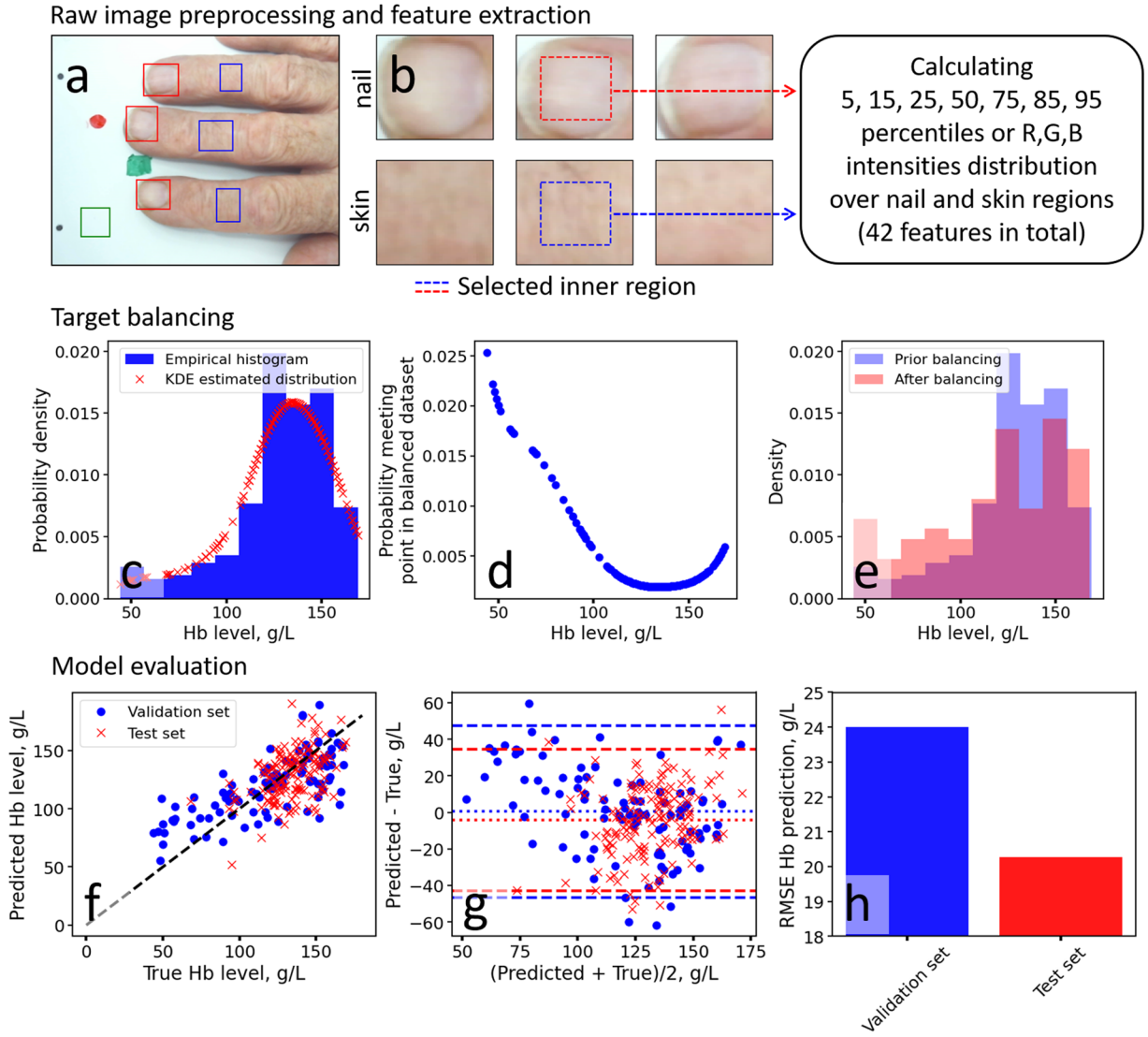

Fig. 5 Summary of the model-building pipeline for the non-invasive blood Hb level prediction from RGB images. (**a**) An exemplary image of patient's hand with marked nails regions (red bounding boxes), skin (blue bounding boxes), and the region used to obtain reference values (green box). (**b**) An example of segmented images of nails and skin. The dotted line shows the subregions of segmented nails and skin images used to calculate the optical descriptors. (**c**) The histogram of the distribution of Hb levels in the original dataset and its kernel density estimation with Gaussian kernel used for dataset balancing. (**d**) Probability distribution for point of the original dataset to be sampled into a balanced subset. (**e**) Comparison of histograms of Hb distribution in the original dataset and balanced subsample. (**f**) Scatter plot for the Hb level predicted by the model from optical descriptors on the Hb level determined using a hematological analyzer for validation and test sets. Dashed line corresponds to the line with identity slope and zero intercept. (**g**) Bland-Altman's plot of the dependence of the difference between the predicted and true Hb level on its half-sum. (**h**) The value of the root-mean-square prediction error of the model on the validation and test data sets.

Hb level for people with different skin tonalities. However, we should note that people with very dark skin color (FP VI) are not represented in our dataset, and such evaluation still needs to be performed.

The obtained values of Hb level prediction errors generally correlate with the levels of accuracy demonstrated by other models (Table 1), yet, we believe that the use of more complex approaches that accurately take into account the color characteristics of the skin and nails can yield higher performance.

Code availability

All code for processing and building the model described in the Usage Notes section is available at https://github.com/biophotonics-msu/photo-haemoglobin.

Received: 7 August 2023; Accepted: 19 September 2024;
Published online: 02 October 2024

References

1. Scott, S. P., Chen-Edinboro, L. P., Caulfield, L. E. & Murray-Kolb, L. E. The Impact of Anemia on Child Mortality: an updated review. *Nutrients* **6**, 5915–5932 (2014).
2. Stevens, G. A. *et al*. Global, regional, and national trends in haemoglobin concentration and prevalence of total and severe anaemia in children and pregnant and non-pregnant women for 1995–2011: a systematic analysis of population-representative data. *The Lancet Global Health* **1**, e16–e25 (2013).
3. Young, M. F. *et al*. Non-invasive hemoglobin measurement devices require refinement to match diagnostic performance with their high level of usability and acceptability. *PLos One* **16**, e0254629 (2021).
4. Goonewardene, M., Shehata, M. & Hamad, A. Anaemia in pregnancy. *Best practice & research Clin. obstetrics & gynaecology* **26**, 3–24 (2012).
5. Haas, J. D. & Brownlie, T. Iron Deficiency and Reduced Work Capacity: A Critical Review of the Research to Determine a Causal Relationship. *The J. nutrition* **131**, 676S–690S (2001).
6. Karakochuk, C. D. *et al*. Measurement and interpretation of hemoglobin concentration in clinical and field settings: a narrative review. *Annals of the new York Acad. Sci.* **1450**, 126–146 (2019).
7. Suner, S. *et al*. Prediction of anemia and estimation of hemoglobin concentration using a smartphone camera. *PLoS One* **16**, e0253495 (2021).
8. Appiahene, P. *et al*. Conjunctival pallor dataset and benchmark for anemia detection in children. *Medicine Nov. Technol. and Devices* **18**, 100244 (2023).
9. Chen, Y., Zhong, K., Zhu, Y. & Sun, Q. Two-stage hemoglobin prediction based on prior causality. *Front. in public health* **10**, 1079389 (2022).
10. Dimauro, G., Camporeale, M. G., Dipalma, A., Guarini, A. & Maglietta, R. Anaemia detection based on sclera and blood vessel colour estimation. *Biomed. Signal Process. Control* **81**, 104489 (2023).
11. Suner, S., McMurdy, J., Jay, G. & Crawford, G. Digital imaging, spectroscopy, and liquid crystals in a hand-held, non-invasive device to determine hemoglobin concentration. *J. Soc. for Inf. Displ.* **15**, 399–407 (2007).
12. Dimauro, G. *et al*. An intelligent non-invasive system for automated diagnosis of anemia exploiting a novel dataset. *Artif.l Intell. Medicine* **136**, 102477 (2023).
13. Collings, S. *et al*. Non-Invasive Detection of Anaemia Using Digital Photographs of the Conjunctiva. *PLoS One* **11**, e0153286 (2016).
14. Park, S. M. *et al*. mHealth spectroscopy of blood hemoglobin with spectral super-resolution. *Optica* **7**, 563–573 (2020).
15. Mitani, A. *et al*. Detection of anaemia from retinal fundus images via deeplearning. *Nat. biomedical engineering* **4**, 18–27 (2020).
16. Zhao, X. *et al*. Deep-Learning-Based Hemoglobin Concentration Prediction and Anemia Screening Using Ultra-Wide Field Fundus Images. *Front. Cell Dev. Biol*. **10** (2022).
17. Babenko, B. *et al*. A deep learning model for novel systemic biomarkers in photographs of the external eye: a retrospective study. *The Lancet Digit. Heal.* **5**, e257–e264 (2023).
18. Causey, M. W. *et al*. Validation of noninvasive hemoglobin measurements using the Masimo Radical-7 SpHb Station. *The Am. journal surgery* **201**, 592–598 (2011).
19. Honnef, G. *et al*. Evaluation of the usefulness of non-invasive serum haemoglobin measurement in a perioperative setting in a prospective observational study. *Sci. Reports* **12**, 9065 (2022).
20. Shamah Levy, T. *et al*. Validation of Masimo Pronto 7 and HemoCue 201 for hemoglobin determination in children from 1 to 5 years of age. *PloS one* **12**, e0170990 (2017).
21. Shah, N., Osea, E. A. & Martinez, G. J. Accuracy of noninvasive hemoglobin and invasive point-of-care hemoglobin testing compared with a laboratory analyzer. *Int. journal of laboratory hematology* **36**, 56–61 (2014).
22. Hornedo-González, K. D. *et al*. Non-invasive hemoglobin estimation for preoperative anemia screening. *Transfusion* **63**, 315–322 (2023).
23. Baulig, W., Seifert, B., Spahn, D. R. & Theusinger, O. M. Accuracy of non-invasive continuous total hemoglobin measurement by Pulse CO-Oximetry in severe traumatized and surgical bleeding patients. *J. clinical monitoring computing* **31**, 177–185 (2017).
24. Yang, S. *et al*. Trends of Hemoglobin Oximetry: Do They Help Predict Blood Transfusion During Trauma Patient Resuscitation? *Anesth. & Analg.* **122** (2016).
25. R G. Mannino *et al*. Clinical and real-world evaluation of a "fingernail selfie" smartphone app for non-invasive, individually-personalized estimation of blood hemoglobin levels. *medRxiv* 2022-12 (2022).
26. Wu, Y., Tanaka, T. & Akimoto, M. Utilization of individual typology angle (ITA) and hue angle in the measurement of skin color on images. *Bioimages* **28**, 1–8 (2020).
27. Clinical and Laboratory Standards Institute. Collection of diagnostic venous blood specimens. (Clinical and Laboratory Standards Institute 2017).
28. Lima-Oliveira, G., Lippi, G., Salvagno, G. L., Picheth, G. & Guidi, G. C. Laboratory diagnostics and quality of blood collection. *J. medical biochemistry* **34**, 288 (2015).
29. Yakimov, B. *et al* Dataset of human skin and fingernails images for non-invasive haemoglobin level assessment. *figshare* https://doi.org/10.6084/m9.figshare.c.6760179 (2024).
30. Hrynaszkiewicz, I., Norton, M. L., Vickers, A. J. & Altman, D. G. Preparing raw clinical data for publication: guidance for journal editors, authors, and peer reviewers. *Bmj* **340** (2010).
31. Hernandez-Andres, J., Lee, R. L. & Romero, J. Calculating correlated color temperatures across the entire gamut of daylight and skylight chromaticities. *Appl. optics* **38**, 5703–5709 (1999).
32. Schindelin, J. *et al*. Fiji: an open-source platform for biological-image analysis. *Nat. Methods* **9**, 676–682 (2012).
33. Zou, H. & Hastie, T. Regularization and Variable Selection Via the Elastic Net. *J. Royal Stat. Soc. Ser. B: Stat. Methodol.* **67**, 301–320 (2005).
34. Pedregosa, F. *et al*. Scikit-learn: Machine learning in Python. *J. machine learning research* **12**, 2825 (2011).
35. Mannino, R. G. *et al*. Smartphone app for non-invasive detection of anemia using only patient-sourced photos. *Nat. Communications* **9**, 4924 (2018).
36. Yılmaz, H., Kızılateş, B. S., Shaaban, F. & Karataş, Z. R. A novel combined deep learning methodology to non-invasively estimate hemoglobin levels in blood with high accuracy. *Med. Eng.g & Phys.* **108**, 103891 (2022).
37. Das, S. *et al*. Smartphone-based non-invasive haemoglobin level estimation by analyzing nail pallor. *Biomed.l Signal Process. and Control* **85**, 104959 (2023).
38. Das, S., Kesarwani, A., Kisku, D. R. & Dalui, M. Non-invasive Haemoglobin Estimation by Observing Nail Color: A PCA based Approach. In *2022 IEEE 6th Conference on Information and Communication Technology (CICT)*, 1–5 (2022).
39. Ahmed, S. & Habib, M. A. Automatic Region of Interest Extraction from Finger Nail Images for Measuring Blood Hemoglobin Level. In *2021 International Conference on Electronics, Communications and Information Technology (ICECIT)*, 1–4 (IEEE, 2021).
40. Asare, J. W., Appiahene, P., Donkoh, E. T. & Dimauro, G. Iron deficiency anemia detection using machine learning models: A comparative study of fingernails, palm and conjunctiva of the eye images. *Eng. Reports* **5**, e12667 (2023).

Acknowledgements
This research was funded by grant from the Moscow government (research project № 2212-19/22). The publication of this manuscript was sponsored by the Moscow Center for Innovative Technologies in Healthcare. Research was performed according to Academic leadership program Priority 2030 proposed by Federal State Autonomous Educational Institution of Higher Education I.M. Sechenov First Moscow State Medical University of the Ministry of Health of the Russian Federation (Sechenov University) and Development Program of the Interdisciplinary Scientific and Educational Schools of Lomonosov Moscow State University "Photonic and Quantum Technologies. Digital medicine".

Author contributions
B.Y., A.S. and E.S. – research design, B.Y., K.B., G.D., I.B. – data collection; I.B. – data preparation and segmentation; Y.S. – full data anonymization; O.P., A.P., L.P. and A.Y. – data curation and validation; B.Y. and E.S. – manuscript draft; all authors revised and corrected the manuscript.

Competing interests
The authors declare no competing interests.

Additional information
Correspondence and requests for materials should be addressed to B.Y. or E.S.

Reprints and permissions information is available at www.nature.com/reprints.

Publisher's note Springer Nature remains neutral with regard to jurisdictional claims in published maps and institutional affiliations.